On the Placement of Latitudes in Iso-Latitude Optimal-Dimensionality Sampling Schemes on the Sphere

Zubair Khalid and Rodney A. Kennedy
Research School of Engineering,
College of Engineering and Computer Science,
The Australian National University,
Canberra, ACT 0200, Australia
Email: {zubair.khalid, rodney.kennedy}@anu.edu.au

***Abstract*—Optimal-dimensionality sampling schemes for band-limited signals (in spherical harmonic degree) on the sphere have been developed such that the number of samples equals the spectral degrees of freedom. These schemes use iso-latitude rings of samples for the computation of the Spherical Harmonic Transform (SHT) to high accuracy. However, the location of the iso-latitude rings had not been fully optimized to attain the highest possible numerical accuracy of the SHT computation. We study the effect of selecting the set of minimal dimensionality set of latitudes from much larger sets distributed according to different measures. In comparison to the other measures on the sphere used in the literature, we show that the placement of iso-latitude rings according to the uniform measure from the larger set allows the most accurate computation of the SHT in the class of (known) optimal-dimensionality sampling schemes. These claims are corroborated with numerical examples.**

***Index Terms*—2-sphere (unit sphere), spherical harmonic transform, sampling, harmonic analysis, spherical harmonics.**

I. Introduction

The development of spherical signal processing techniques finds applications in various fields of science and engineering, where signals are naturally defined on the sphere. These applications include geodesy [1], planetary science [2], electromagnetic inverse problems [3], medical imaging [4], 3D beamforming [5] and wireless channel modeling [6], to name a few. Many signal processing techniques have been developed to analyze the signal defined on the sphere (e.g., [7]–[10]). At the core of these developments, the signal is analyzed either in the spatial domain or spectral domain. The spectral domain is formed through the spherical harmonic transform (SHT), which is the well-known counterpart of the Fourier transform for signals on the sphere [11]. Clearly, the ability to accurately compute the spherical harmonic transform of sampled (discretized) signal is of significant importance. Furthermore, it is desirable that the methods to compute SHT require fewer samples on the sphere and are supported by computationally efficient algorithms [12], [13].

Many sampling schemes on the sphere, supported by accurate and fast SHT methods, have been proposed in the literature (e.g., see [12]–[15] and references therein). Common to the literature, we focus on the sampling schemes which support accurate computation of the SHT for signals band-limited at degree L (defined in Section II-B). Recently, the sampling scheme, referred as optimal-dimensionality sampling scheme, that allows the accurate computation of SHT has been proposed [12]. This scheme only requires the optimal (minimal) number of samples, L^2, given by the degrees of freedom in spectral domain, in order to compute spherical harmonic transform accurately. In comparison, the equiangular sampling schemes, based on the sampling theorem, although supporting exact quadrature require twice ($2L^2$) [13] or four times ($4L^2$) [14] of the optimal number of samples. The optimal-dimensionality sampling scheme belongs to the class of iso-latitude sampling schemes (e.g., [13], [14]), where the samples along longitude are taken over iso-latitude rings. Furthermore, the iso-latitude structure of the sampling scheme allows separation of variables in the computation of the SHT, which results in a SHT with reduced computational complexity.

In optimal-dimensionality sampling schemes, the L iso-latitude rings are placed according to uniform measure along latitude, which is shown to achieve more accurate SHT computation of a signal band-limited at degree L compared to the case when the L rings are placed along latitude according to different measures, such as based on the sine and tangent of the latitude [16]. The placement of rings according to the uniform measure, although an intuitive choice and supports accurate spherical harmonic transform, may not be an optimal choice to place the iso-latitude rings of samples. In this context, we answer the following questions (mathematically formulated in Section III-C) in this work:

- Is the SHT computational accuracy *significantly* improved if we optimally select our L iso-latitude rings from a larger set of $M \gg L$ latitudes distributed with uniform measure in latitude?
- Is the SHT computational accuracy *significantly* improved if the L iso-latitude rings are selected according to other non-uniform measures developed in the literature?

978-1-4799-5255-7/14/$31.00 ©2014 IEEE

In addressing these questions, we organize the paper as follows. In Section II, we present the mathematical background for signals on the sphere. In Section III, we review the optimal-dimensionality sampling scheme [12] and formulate the research questions considered in this work. In Section IV, we develop a method to optimally place L iso-latitude rings from a set of $M \gg L$ samples along latitude, where the M samples are distributed according to some defined measure on the sphere. We also analyze the effect of placement of samples according to different measures (adopted in the literature) on the accuracy of SHT. We show that the placement of iso-latitude rings according to the uniform measure allows the most accurate computation of SHT associated with the optimal-dimensionality sampling scheme. Finally, we summarize the findings in Section V.

II. Mathematical Preliminaries

In this section we review the mathematical background for signals and harmonic analysis on the sphere.

A. Signals on the Sphere

We consider complex valued square integrable functions $f(\theta, \phi)$, defined on a unit sphere $\mathbb{S}^2 \triangleq \{\mathbf{u} \in \mathbb{R}^3 \colon |\mathbf{u}| = 1\}$, where $\theta \in [0, \pi]$ denotes the co-latitude that is measured from positive z-axis, $\phi \in [0, 2\pi)$ denotes the longitude that is measured from the positive x-axis in the $x-y$ plane and $|\cdot|$ denotes the Euclidian norm.

The set of square integrable complex valued functions defined on $\mathbb{S}^2$ forms a complete Hilbert space $L^2(\mathbb{S}^2)$ with the inner product defined for two functions f and h defined on $\mathbb{S}^2$ as [17]

$$\langle f, h \rangle \triangleq \int_{\mathbb{S}^2} f(\theta, \phi) \overline{h(\theta, \phi)} \sin\theta \, d\theta \, d\phi, \tag{1}$$

where $\sin\theta \, d\theta \, d\phi$ denotes the differential area element on the sphere, $\overline{(\cdot)}$ denotes the complex conjugate and the integration is carried out over the sphere. The inner product in (1) induces a norm $\|f\| \triangleq \langle f, f \rangle^{1/2}$. The functions with finite induced norm are referred as signals on the sphere.

B. Spherical Harmonics

The Hilbert space $L^2(\mathbb{S}^2)$ is separable and the spherical harmonic functions form the archetype complete orthonormal set of basis functions. The spherical harmonic function (or spherical harmonic for short), $Y_\ell^m(\theta, \phi)$, for degree $\ell \geq 0$ and order $|m| \leq \ell$ is defined as [11]

$$Y_\ell^m(\theta, \phi) = N_\ell^m P_\ell^m(\cos\theta) \, e^{im\phi}, \tag{2}$$

with $N_\ell^m \triangleq \sqrt{\frac{2\ell+1}{4\pi} \frac{(\ell-m)!}{(\ell+m)!}}$ is the normalization factor such that $\langle Y_\ell^m, Y_p^q \rangle = \delta_{\ell,p} \delta_{m,q}$, where $\delta_{m,q}$ is the Kronecker delta function: $\delta_{m,q} = 1$ for $m = q$ and is zero otherwise. $P_\ell^m(x)$ is the associated Legendre function defined for degree ℓ and order $0 \leq m \leq \ell$ as

$$P_\ell^m(x) = \frac{(-1)^m}{2^\ell \ell!} (1-x^2)^{m/2} \frac{d^{\ell+m}}{dx^{\ell+m}} (x^2-1)^\ell$$
$$P_\ell^{-m}(x) = (-1)^m \frac{(\ell-m)!}{(\ell+m)!} P_\ell^m(x),$$

for $|x| \leq 1$.

By completeness of spherical harmonics, any signal $f \in L^2(\mathbb{S}^2)$ can be expanded as

$$f(\theta, \phi) = \sum_{\ell=0}^{\infty} \sum_{m=-\ell}^{\ell} (f)_\ell^m Y_\ell^m(\theta, \phi), \tag{3}$$

where

$$(f)_\ell^m \triangleq \langle f, Y_\ell^m \rangle = \int_{\mathbb{S}^2} f(\theta, \phi) \overline{Y_\ell^m(\theta, \phi)} \sin\theta \, d\theta \, d\phi \tag{4}$$

is the spherical harmonic coefficient of degree ℓ and order m.

III. Problem Formulation

We consider the problem of how to compute the spherical harmonic transform, that is, the spherical harmonic coefficients given in (4), of a band-limited discretized (sampled) signal on the sphere. The signal $f \in L^2(\mathbb{S}^2)$ is defined to be band-limited at degree L if $(f)_\ell^m = 0$ for $\ell \geq L$. The spherical harmonic transform (SHT) of a signal f band-limited to degree L can be expressed as

$$f(\theta, \phi) = \sum_{\ell=0}^{L-1} \sum_{m=-\ell}^{\ell} (f)_\ell^m Y_\ell^m(\theta, \phi), \tag{5}$$

where the summation over degree ℓ in (3) is limited to $L-1$.

There exist many sampling schemes on the sphere which allow accurate computation of the spherical harmonic transform of a band-limited signal [12]–[14]. In this work, we consider the recently developed sampling scheme on the sphere [12], which was referred to as an optimal-dimensionality sampling scheme as it requires the minimum number of samples, L^2, on the sphere to accurately compute the spherical harmonic transform, in comparison to the schemes based on sampling theorems proposed in [14] and [13], which require $4L^2$ and $2L^2$ samples, respectively. We refer the reader to [12] and [13] for a detailed comparison of different sampling schemes proposed in literature.

A. Optimal-Dimensionality Sampling Scheme

We review the iso-latitude sampling scheme on the sphere proposed in [12]. Let such a sampling scheme be denoted by $\mathfrak{S}(L)$ that consists of L iso-latitude rings of samples (where L is the band-limit). Let the indexed vector

$$\boldsymbol{\theta} \triangleq [\theta_0, \, \theta_1, \, \ldots, \, \theta_{L-1}]^T, \tag{6}$$

represent L (possibly) arbitrary, ordered and distinct, points along θ that describes the L iso-latitude rings. We discuss the precise location of these rings of sample points later in the paper.

For discretization along ϕ, we consider $2k+1$ equally spaced sampling points along ϕ for each $\theta_k \in \boldsymbol{\theta}$. Define $\boldsymbol{\phi}^k$ be a vector of $2k+1$ equally spaced sampling points along ϕ in the ring placed at θ_k, given by

$$\boldsymbol{\phi}^k \triangleq \big[0, \Delta_k, 2\Delta_k, \ldots, (2k)\Delta_k\big], \quad \Delta_k = \frac{2\pi}{2k+1}. \tag{7}$$

The vectors $\boldsymbol{\theta}$ and $\boldsymbol{\phi}^k$, for every k, describe the structure of the sampling scheme $\mathfrak{S}(L)$, where we note that the number of points, $2k+1$, in ring k varies precisely in the way that the total number of points is L^2.

B. Computation of Spherical Harmonic Transform

We review the SHT, developed in [12], to compute the spherical harmonic coefficients $(f)_\ell^m$ of a band-limited signal f sampled over the sampling scheme $\mathfrak{S}(L)$. Define a vector

$$\mathbf{g}_m \triangleq \left[G_m(\theta_{|m|}), G_m(\theta_{|m|+1}), \ldots, G_m(\theta_{L-1})\right]^T, \tag{8}$$

for order $|m| < L$, where $G_m(\theta_k)$ is defined for each $\theta_k \in \boldsymbol{\theta}$ as

$$\begin{aligned} G_m(\theta_k) &\triangleq \int_0^{2\pi} f(\theta_k, \phi) e^{-im\phi} d\phi \\ &= 2\pi \sum_{\ell=m}^{L-1} (f)_\ell^m \tilde{P}_\ell^m(\theta_k). \end{aligned} \tag{9}$$

Here $\tilde{P}_\ell^m(\theta) \triangleq Y_\ell^m(\theta, 0)$ denotes the scaled associated Legendre functions. By defining a vector $\mathbf{f}_m$ containing spherical harmonic coefficients of order $|m| < L$ given by

$$\mathbf{f}_m = \left[(f)_{|m|}^m, (f)_{|m|+1}^m, \ldots, (f)_{L-1}^m\right]^T, \tag{10}$$

and a matrix $\mathbf{P}_m$ as

$$\mathbf{P}_m \triangleq 2\pi \begin{pmatrix} \tilde{P}_{|m|}^m(\theta_{|m|}) & \tilde{P}_{|m|+1}^m(\theta_{|m|}) & \cdots & \tilde{P}_{L-1}^m(\theta_{|m|}) \\ \tilde{P}_{|m|}^m(\theta_{|m|+1}) & \tilde{P}_{|m|+1}^m(\theta_{|m|+1}) & \cdots & \tilde{P}_{L-1}^m(\theta_{|m|+1}) \\ \vdots & \vdots & \ddots & \vdots \\ \tilde{P}_{|m|}^m(\theta_{L-1}) & \tilde{P}_{|m|+1}^m(\theta_{L-1}) & \cdots & \tilde{P}_{L-1}^m(\theta_{L-1}) \end{pmatrix}, \tag{11}$$

we write $\mathbf{g}_m$ as

$$\mathbf{g}_m = \mathbf{P}_m \mathbf{f}_m, \tag{12}$$

where the vector $\mathbf{g}_m$ is given in (8). Using the formulation in (12), the spherical harmonic coefficients in a vector $\mathbf{f}_m$ for each $|m| < L$ can be computed provided the vector $\mathbf{g}_m$ is computed correctly and the matrix $\mathbf{P}_m$ is invertible.

By taking samples of the signal over the grid $\mathfrak{S}(L)$, the vector $\mathbf{g}_m$ can be accurately computed by taking FFT of the samples in each ring along longitude [12]. However, the invertibility of the matrix $\mathbf{P}_m$ for each $|m| < L$ depends on the sample positions in the vector $\boldsymbol{\theta}$, where the iso-latitude rings are placed. The sample positions in the vector $\boldsymbol{\theta}$ should be chosen such that each of the matrices $\mathbf{P}_m$, which depends on last $L-m$ samples of the vector $\boldsymbol{\theta}$, is well-conditioned.

The simplest choice is to use the equiangular set (with uniform measure along θ) of samples given by

$$\Theta^1(L) = \left\{ \frac{\pi(2t+1)}{2L-1} \right\}, \quad t = 0, 1, \ldots, L-1, \tag{13}$$

for the placement of the rings, where rings are placed such that those with more samples along longitude are generally placed nearer to the equator ($\theta = \pi/2$) [12]. For such an arrangement, the vector $\boldsymbol{\theta}$ for band-limit L is given by

$$\boldsymbol{\theta} \triangleq \left[\pi, \frac{\pi}{2L-1}, \frac{\pi(2L-3)}{2L-1}, \frac{3\pi}{2L-1}, \ldots, \frac{\pi(2\lfloor \frac{L-1}{2} \rfloor + 1)}{2L-1}\right]^T. \tag{14}$$

As an example, Figure 1 shows the sampling grid $\mathfrak{S}(L)$ for $L = 16$ and $\boldsymbol{\theta}$ given as in (14).

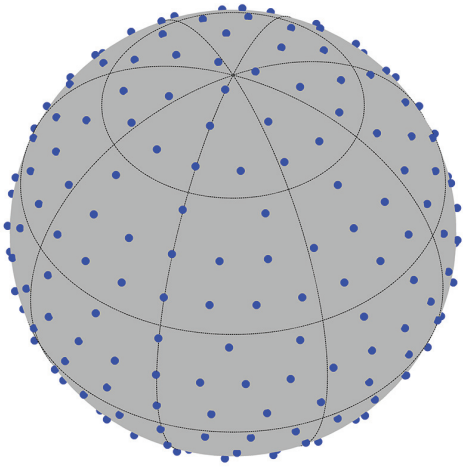

(a) North Pole View

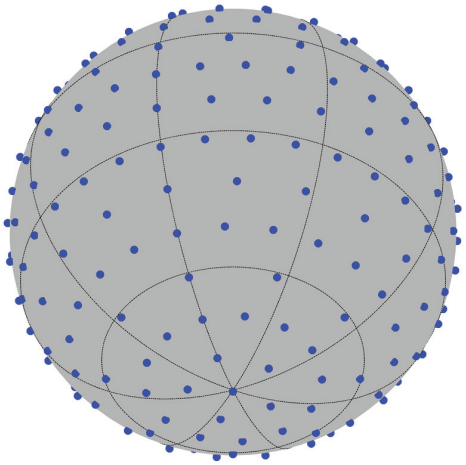

(b) South Pole View

Fig. 1: The sampling scheme $\mathfrak{S}(L)$ for the representation of the signal band-limited at $L = 16$. The sample positions $\boldsymbol{\theta}$ along latitude are given in (14). The samples on the sphere are shown with a view from (a) North Pole and (b) South Pole.

C. Research Questions under Consideration

The placement of rings with equal angular spacing, although an attractive choice, may not be appropriate as the matrix $\mathbf{P}^m$

for some $|m| < L$ can become ill-conditioned [12]. In order to ensure the invertibility of the matrix $\mathbf{P}_m$ for each m, the sample positions in $\boldsymbol{\theta}$ has been constructed from the samples in the set $\Theta^1(L)$ given by (13) by minimizing the condition number (ratio of largest eigenvalue to the smallest eigenvalue) of matrix $\mathbf{P}^m$ for each $m \in \{L-2, L-3, \ldots, 0\}$. Such optimized placement of samples along latitude significantly improves the conditioning of the matrices, and consequently allows an accurate computation of spherical harmonic coefficients. However, the minimization of condition number only chooses from this set of L samples, which motivates us to explore the possibility of further improvement in the condition number of the matrix $\mathbf{P}^m$ for each $|m| < L$, if the L sample positions along latitude are obtained from a larger set of samples distributed along latitude. In this context, we seek to answer to the following research question.

> *Q1: How does the accuracy of the SHT improve if we choose sample positions to construct vector $\boldsymbol{\theta}$ from a larger set $\Theta^1(M)$, $M \gg L$ of equiangular samples along latitude such that condition number of the matrix $\mathbf{P}_m$ for each $m < L$ is minimized?*

Furthermore, the equiangular samples in the set $\Theta^1(L)$ are placed along latitude θ according to a uniform measure $d\theta$. Alternatively, the samples along co-latitude can be placed according to different measures such as the standard spherical measure $\sin\theta\, d\theta$ and the measure $|\tan\theta|^{1/3} d\theta\, d\phi$, which is used in the recovery of sparse band-limited signal [16]. It has been demonstrated that the placement of sample positions along latitude with the uniform measure $d\theta$ results in a more accurate computation of SHT, in comparison to the placement of samples along latitude according to the measures $\sin\theta\, d\theta$ and $|\tan\theta|^{1/3} d\theta$. This further guides the need to address the following research question in this work:

> *Q2: If the samples in the larger set are taken according to other measures such as $\sin\theta\, d\theta$ and $|\tan\theta|^{1/3} d\theta$, what is the distribution of samples in the vector $\boldsymbol{\theta}$ (which minimizes the condition number of the matrix $\mathbf{P}_m$ for each $m < L$) and does such an arrangement of sample positions along latitude improve the accuracy of the SHT computation?*

IV. Optimal Placement of Samples

We analyze the construction of the optimized sample positions in a vector $\boldsymbol{\theta}$ from a large set of $M \gg L$ samples along latitude, where the M samples are distributed according to different measures. In addition to the uniform measure $d\theta$ [12], [13], [18], the other measures considered in the literature are the standard measure $\sin\theta\, d\theta$ and tangent measure $|\tan\theta|^{1/3} d\theta$ [16]. We first define the set of sample points along latitude with different measures. Define $\Theta^2(M) = \left\{\Theta_t^2\right\}$ and $\Theta^3(M) = \left\{\Theta_t^3\right\}$ for $t = 0, 1, \ldots, M-1$ as sets of M samples along co-latitude, where samples are placed according to the measures $\sin\theta\, d\theta$ and $|\tan\theta|^{1/3} d\theta$, respectively. The sets $\Theta^2(M)$ and $\Theta^3(M)$ are formed by choosing $\Theta_0^2 = \Theta_0^3 = \pi$ (South Pole) and using the following relation between the consecutive samples:

$$\int_{\Theta_t^2}^{\Theta_{t-1}^2} \sin\theta\, d\theta = \frac{1}{L}\int_0^{\pi} \sin\theta\, d\theta = \frac{2}{L}, \tag{15}$$

$$\int_{\Theta_t^3}^{\Theta_{t-1}^3} |\tan\theta|^{1/3} d\theta = \frac{1}{L}\int_0^{\pi} |\tan\theta|^{1/3} d\theta = \frac{2\pi}{L\sqrt{3}}, \tag{16}$$

for $t = 1, 2, \ldots, M-1$. The samples in the set $\Theta^2(M)$ can also be formed as $\Theta_t^2 = \arccos z_t$ where $z_t = 2t/M - 1$ for $t = 0, 1, \ldots, M-1$. Since $\tan\theta$ is discontinuous at $\theta = \pi/2$, we note that the samples with the measure $|\tan\theta|^{1/3} d\theta$ can only be determined using the formulation in (16).

A. Optimal Sample Placement — Method

We propose to choose sample positions $\boldsymbol{\theta}$ from a large set of M samples using the following method:

- Choose θ_{L-1} (where the ring of $2L-1$ samples is placed) from the set of M samples as the farthest sample ring from the poles.
- For each $m = L-2, L-3, \ldots, 0$, choose θ_m from the set of M samples, such that the condition number of the matrix $\mathbf{P}^m$ is minimized.

Since the proposed method minimizes the condition number of the matrix $\mathbf{P}_m$ for each $m < L$, we refer to the proposed method as an "optimal sample placement method". We use the term "optimized sample positions" to refer to the sample positions obtained by applying this method. In optimal placement method, the sequential placement of rings ensures that the matrix $\mathbf{P}^m$ for each m is well-conditioned (or optimally conditioned), resulting in a more accurate computation of the SHT of a band-limited signal.

B. Optimal Sample Placement — Analysis

We analyze the construction of the vector $\boldsymbol{\theta}$ from the set of M samples distributed along latitude with respect to different measures. In our analysis, we choose band-limit $L = 128$ and number of samples $M = 20\,L$, distributed along latitude according to different measures. The optimal sample placement method is applied to determine the optimized sample positions $\boldsymbol{\theta}$ from each of the set $\Theta^1(M)$, $\Theta^2(M)$ and $\Theta^3(M)$. Let the optimized sample positions be denoted by $\boldsymbol{\theta}^1$, $\boldsymbol{\theta}^2$ and $\boldsymbol{\theta}^3$, obtained from the sets $\Theta^1(M)$, $\Theta^2(M)$ and $\Theta^3(M)$, respectively.

The optimized sample positions vector $\boldsymbol{\theta}^1$ is shown in Fig. 2(a) and the condition number, denoted by κ_m, of the matrix $\mathbf{P}^m$, constructed with optimized sample positions $\boldsymbol{\theta}^1$ is plotted in Fig. 2(b) for different values of $0 \le m < L$. Similar plots for the optimized sample positions contained in $\boldsymbol{\theta}^2$ and $\boldsymbol{\theta}^3$ are shown in Fig. 3 and Fig. 4, respectively. We note that the optimized sample positions vector $\boldsymbol{\theta}$ obtained for each of these different sets yield well-conditioned matrices, which is due to the fact that there are more samples, M, in each of the set than the number of samples, L, required to construct optimized sample positions. This is a different finding to the analysis presented in [12], where only L samples in each of the set $\Theta^2(L)$ and $\Theta^3(L)$ are taken along latitude. The comparison

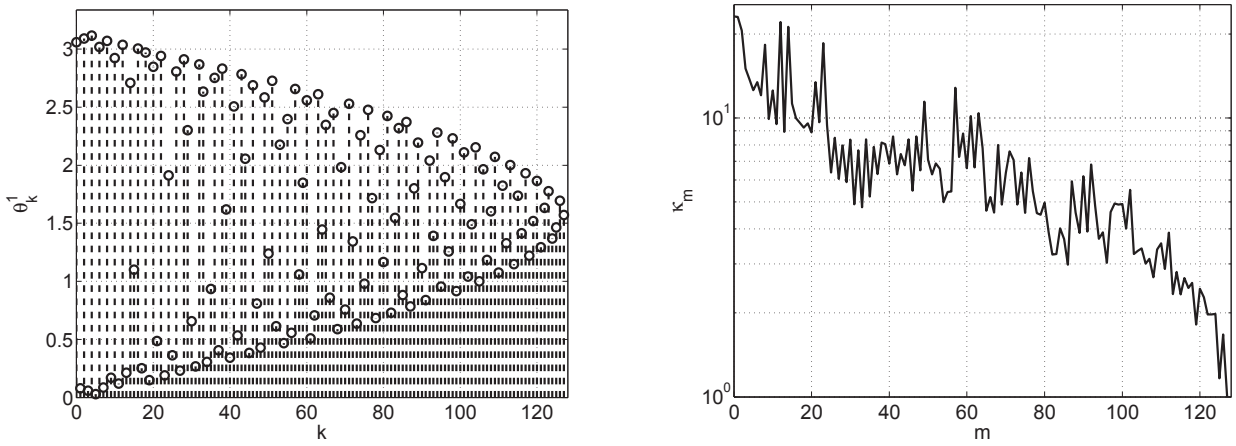

(a) (b)

Fig. 2: (a) The optimized sample positions vector $\boldsymbol{\theta}^1$ for $L = 128$, obtained from the set $\Theta^1(20L)$ with samples taken along latitude according to the measure $d\theta$. (b) The condition number, denoted by κ_m, of the matrix $\mathbf{P}^m$, constructed with optimized sample positions $\boldsymbol{\theta}^1$.

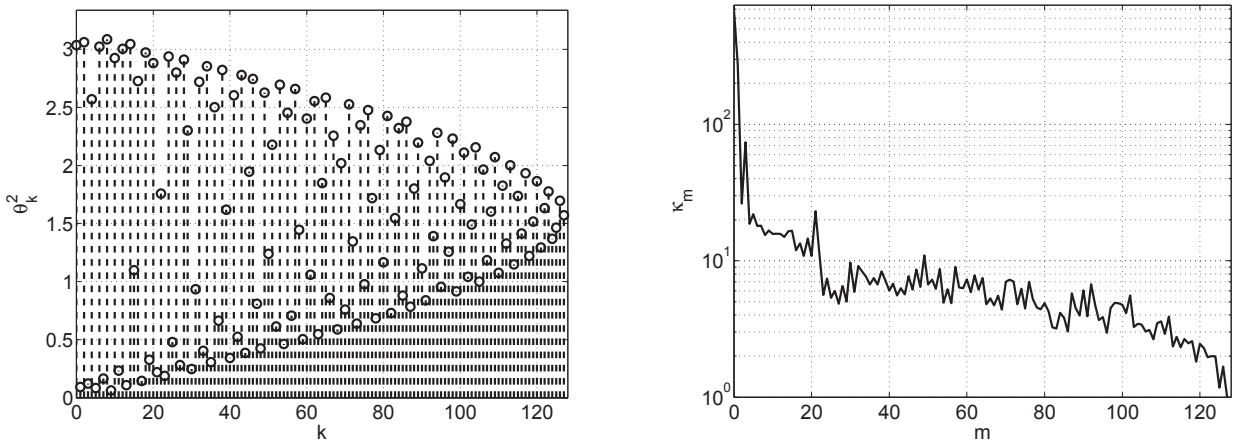

(a) (b)

Fig. 3: (a) The optimized sample positions vector $\boldsymbol{\theta}^2$ for $L = 128$, obtained from the set $\Theta^2(20L)$ with samples taken along latitude according to the measure $\sin\theta\, d\theta$. (b) The condition number, denoted by κ_m, of the matrix $\mathbf{P}^m$, constructed with optimized sample positions $\boldsymbol{\theta}^2$.

of the plots of the condition number κ_m in Fig. 2(b), Fig. 3(b) and Fig. 4(b) also suggests the optimized sample positions $\boldsymbol{\theta}^1$ and $\boldsymbol{\theta}^2$ comparatively attain lower condition numbers.

For more detailed analysis, we plot the maximum of the condition number, denoted by $\max(\kappa_m)$ over $0 \leq m < L$ for different values of the band-limit $16 \leq L \leq 256$ in Fig. 5 and for optimized sample positions obtained from different sets as indicated. As we noted earlier, it can be observed again that the matrix $\mathbf{P}^m$ for each $0 \leq m < L$, constructed with the sample positions $\boldsymbol{\theta}^3$ have the smallest $\max(\kappa_m)$ over $0 \leq m < L$ for the given band-limit. Furthermore, the sample positions $\boldsymbol{\theta}^2$, obtained from the set $\Theta^2(M)$ with samples taken according to standard measure on the sphere $\sin\theta\, d\theta$, have largest $\max(\kappa_m)$.

Remark 1: This finding is consistent with the results in [16], where it has been proved in that a sparse band-limited signal can be recovered from fewer measurements if samples are drawn from the measure $|\tan\theta|^{1/3} d\theta d\phi$, compared to sampling with respect to the uniform measure $d\theta d\phi$, which in turn has been shown by [18] to require fewer samples than sampling with respect to the measure $\sin\theta\, d\theta$.

In Fig. 5, we also plot the maximum of the condition number $\max(\kappa_m)$ for the case when optimized sample positions in a vector $\boldsymbol{\theta}$ are determined by applying the optimal sample placement method on the set $\Theta^1(L)$ (set of *only* L points along latitude distributed according to uniform measure). We refer to such sample positions vector as the optimal sample positions vector, denoted by $\tilde{\boldsymbol{\theta}}$, which is determined by applying the

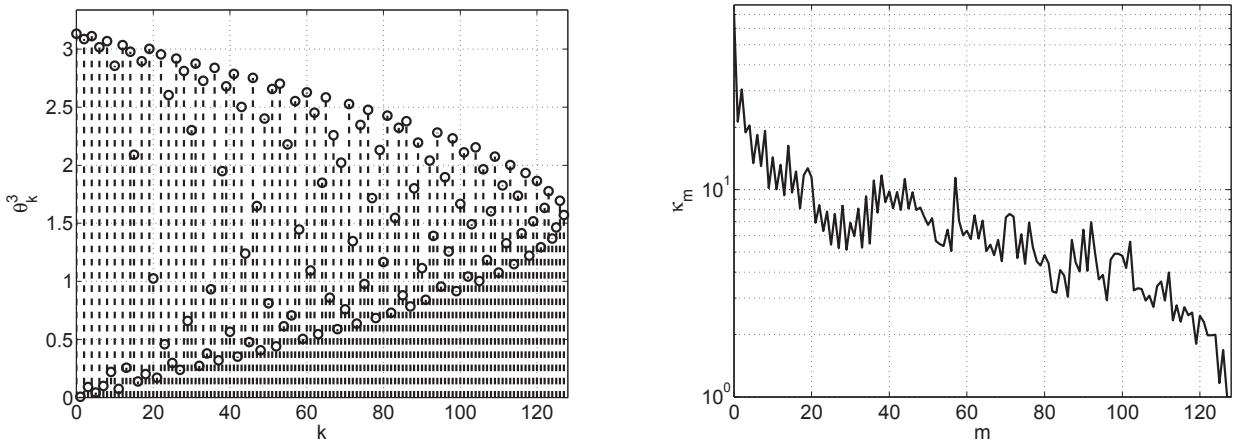

(a) (b)

Fig. 4: (a) The optimized sample positions vector $\boldsymbol{\theta}^3$ for $L = 128$, obtained from the set $\Theta^3(20L)$ with samples taken along latitude according to the measure $|\tan\theta|^{1/3}d\theta$. (b) The condition number, denoted by κ_m, of the matrix $\mathbf{P}^m$, constructed with optimized sample positions $\boldsymbol{\theta}^3$.

optimal sample placement method on the set $\Theta^1(L)$. It is interesting to note that optimized sample positions vector obtained from set $\Theta^1(L)$ yields even lower $\max(\kappa_m)$.

Remark 2: The analysis suggests that the optimized sample positions $\tilde{\boldsymbol{\theta}}$ obtained from the set of only L samples, taken according to uniform measure $d\theta$, is the best choice (in terms of numerical accuracy of the SHT) to place the rings in the optimal-dimensionality sampling scheme.

We carry out further analysis to justify that the placement of sample positions with uniform measure is the best choice to place iso-latitude rings. We show that the optimized sample positions obtained from either of the sets $\Theta^1(M)$, $\Theta^2(M)$ or $\Theta^3(M)$ by applying the optimal sample placement method approaches optimal sample positions vector $\tilde{\boldsymbol{\theta}}$ as $M \to \infty$ (or $M \gg L$). We determine optimized sample positions $\boldsymbol{\theta}^1$, $\boldsymbol{\theta}^2$, $\boldsymbol{\theta}^3$ and optimal sample positions $\tilde{\boldsymbol{\theta}}$ for $L = 64$ and $M = 2560$ and $M = 5120$. The absolute difference between the sorted $\boldsymbol{\theta}^1$ (or $\boldsymbol{\theta}^2$, $\boldsymbol{\theta}^3$) and sorted $\tilde{\boldsymbol{\theta}}$ is shown in Fig. 6(a) and (b) for $M = 2560$ and $M = 5120$, where it is evident that each of the optimized sample positions $\boldsymbol{\theta}^i$ for $i = 1, 2, 3$, obtained from their respective sets distributed along latitude with different measures, well-approximates the optimal sample positions $\tilde{\boldsymbol{\theta}}$ and the approximation becomes better if more samples are taken in each of the sets. Furthermore, we emphasize here again that the condition number of the matrix $\mathbf{P}^m$, constructed with optimal sample positions $\tilde{\boldsymbol{\theta}}$, for all $0 \leq m < L$, is as small as possible, resulting in a more accurate computation of the SHT.

Remark 3: Since the optimized sample positions $\boldsymbol{\theta}^1$, $\boldsymbol{\theta}^2$, $\boldsymbol{\theta}^3$ are distributed according to uniform measure on the sphere for large $M \gg L$, we note that the placement of iso-latitude rings according to the uniform measure $d\theta$ is an optimal choice, in comparison to the other measures such as $\sin\theta\, d\theta$ and $|\tan\theta|^{1/3}d\theta$ on the sphere, for the accurate computation of the SHT.

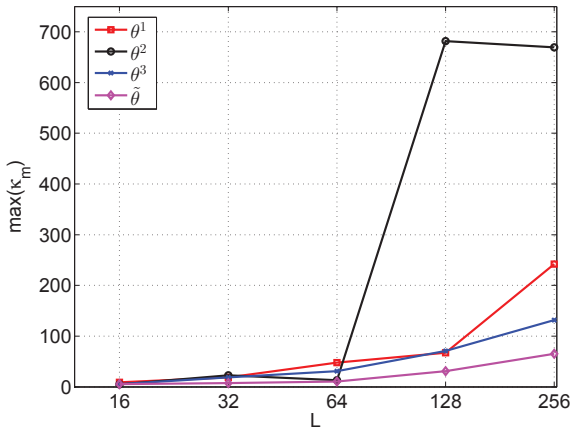

Fig. 5: The maximum of the condition number, $\max(\kappa_m)$ of the matrix $\mathbf{P}^m$ over $0 \leq m < L$ for band-limit $16 \leq L \leq 256$, where the matrix $\mathbf{P}^m$ is constructed with the optimized sample positions $\boldsymbol{\theta}^i$, $i = 1, 2, 3$, or optimal sample positions $\tilde{\boldsymbol{\theta}}$.

V. Conclusions

In this work, we have investigated the use of different choices to place the samples in an optimal-dimensionality sampling scheme — one where the total number of samples is L^2. For the accurate representation of a signal band-limited at L, the optimal-dimensionality scheme is composed of L iso-latitude rings of samples. Since the accuracy of the spherical harmonic transform depends on the sample positions along latitude, where the iso-latitude rings are placed, we have analyzed the effect of placement of samples according to different measures on the accuracy of SHT. We have developed a method to determine L optimal sample positions from a

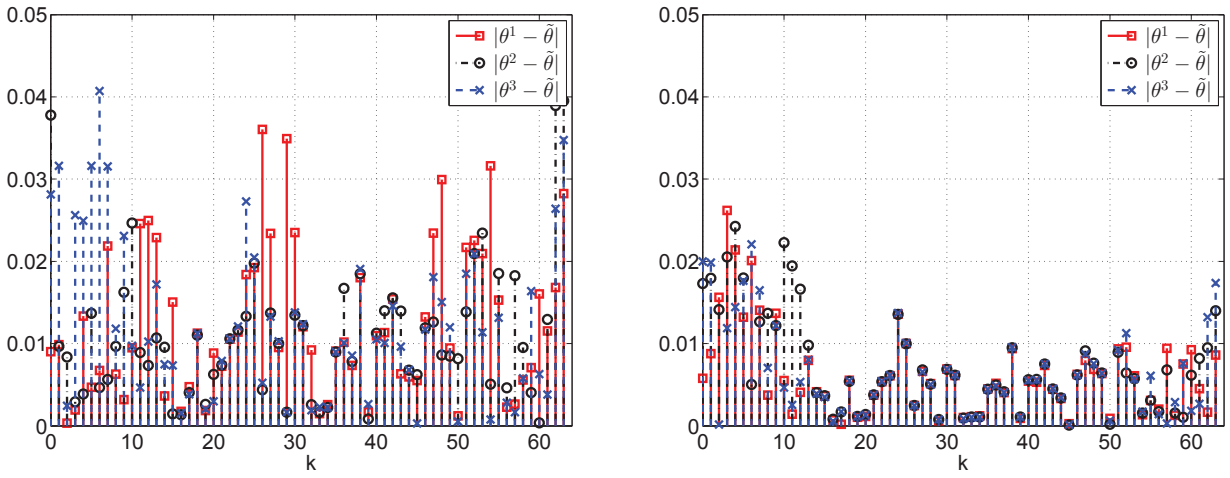

(a) $M = 2560$ (b) $M = 5210$

Fig. 6: The absolute difference between the sorted $\boldsymbol{\theta}^1$ (or $\boldsymbol{\theta}^2$, $\boldsymbol{\theta}^3$) and sorted $\tilde{\boldsymbol{\theta}}$ (the legend indicates the quantity along the vertical axis) for (a) $M = 2560$ and (b) $M = 5120$. The small difference indicates that each of the optimized sample positions $\boldsymbol{\theta}^i$ for $i = 1, 2, 3$, well-approximates the optimal sample positions $\tilde{\boldsymbol{\theta}}$. Note that the approximation becomes better for $M = 5120$.

given set of $M \gg L$ samples along latitude, which is used to evaluate the effect of placement of samples according to different measures on the accuracy of SHT. In comparison to the other measures on the sphere used in the literature, we have shown that the placement of iso-latitude rings according to the uniform measure allows the most accurate computation of spherical harmonic transform.

REFERENCES

[1] F. J. Simons, F. A. Dahlen, and M. A. Wieczorek, "Spatiospectral concentration on a sphere," *SIAM Rev.*, vol. 48, no. 3, pp. 504–536, 2006.

[2] P. Audet, "Directional wavelet analysis on the sphere: Application to gravity and topography of the terrestrial planets," *J. Geophys. Res.*, vol. 116, Feb. 2011.

[3] D. Colton and R. Kress, *Inverse Acoustic and Electromagnetic Scattering Theory*, 2nd ed. Berlin: Springer-Verlag, 1998.

[4] M. K. Chung, K. M. Dalton, L. Shen, A. C. Evans, and R. J. Davidson, "Weighted fourier series representation and its application to quantifying the amount of gray matter," *IEEE Trans. Med. Imag.*, vol. 26, no. 4, pp. 566–581, Apr. 2007.

[5] D. B. Ward, R. A. Kennedy, and R. C. Williamson, "Theory and design of broadband sensor arrays with frequency invariant far-field beam patterns," *J. Acoust. Soc. Am.*, vol. 97, no. 2, pp. 1023–1034, Feb. 1995.

[6] T. S. Pollock, T. D. Abhayapala, and R. A. Kennedy, "Introducing space into MIMO capacity calculations," *J. Telecommun. Syst.*, vol. 24, no. 2, pp. 415–436, Oct. 2003.

[7] Z. Khalid, S. Durrani, P. Sadeghi, and R. A. Kennedy, "Spatio-spectral analysis on the sphere using spatially localized spherical harmonics transform," *IEEE Trans. Signal Process.*, vol. 60, no. 3, pp. 1487–1492, Mar. 2012.

[8] J. D. McEwen, M. P. Hobson, and A. N. Lasenby, "Optimal filters on the sphere," *IEEE Trans. Signal Process.*, vol. 56, no. 8, pp. 3813–3823, Aug. 2008.

[9] P. Sadeghi, R. A. Kennedy, and Z. Khalid, "Commutative anisotropic convolution on the 2-sphere," *IEEE Trans. Signal Process.*, vol. 60, no. 12, pp. 6697–6703, Dec. 2012.

[10] B. T. T. Yeo, W. Ou, and P. Golland, "On the construction of invertible filter banks on the 2-sphere," *IEEE Trans. Image Process.*, vol. 17, no. 3, pp. 283–300, Mar. 2008.

[11] R. A. Kennedy and P. Sadeghi, *Hilbert Space Methods in Signal Processing*. Cambridge, UK: Cambridge University Press, Mar. 2013.

[12] Z. Khalid, R. A. Kennedy, and J. D. McEwen, "An optimal-dimensionality sampling scheme on the sphere with fast spherical harmonic transforms," *IEEE Trans. Signal Process.*, vol. 62, no. 17, pp. 4597–4610, Sep. 2014.

[13] J. D. McEwen and Y. Wiaux, "A novel sampling theorem on the sphere," *IEEE Trans. Signal Process.*, vol. 59, no. 12, pp. 5876–5887, Dec. 2011.

[14] J. R. Driscoll and D. M. Healy, Jr., "Computing Fourier transforms and convolutions on the 2-sphere," *Adv. Appl. Math.*, vol. 15, no. 2, pp. 202–250, Jun. 1994.

[15] D. M. Healy, Jr., D. Rockmore, P. J. Kostelec, and S. S. B. Moore, "FFTs for the 2-sphere - improvements and variations," *J. Fourier Anal. and Appl.*, vol. 9, pp. 341–385, 2003.

[16] N. Burq, S. Dyatlov, R. Ward, and M. Zworski, "Weighted eigenfunction estimates with applications to compressed sensing," *SIAM J. Math. Anal.*, vol. 44, no. 5, pp. 3481–3501, 2012.

[17] R. A. Kennedy, T. A. Lamahewa, and L. Wei, "On azimuthally symmetric 2-sphere convolution," *Digital Signal Processing*, vol. 5, no. 11, pp. 660–666, Sep. 2011.

[18] H. Rauhut and R. Ward, "Sparse recovery for spherical harmonic expansions," in *Proc. SampTA 2011, Singapore*, 2011.